
A FUNCTION-SPACE STABILITY BOUNDARY FOR GENERALIZATION IN INTERPOLATING LEARNING SYSTEMS

Ronald Katende

Department of Mathematics

Kabale University

Kikungiri Hill, Katuna Road, 317, Kabale, Uganda

rkatende@kab.ac.ug

ABSTRACT

Modern learning systems often interpolate training data while still generalizing well, yet it remains unclear when algorithmic stability explains this behavior. We model training as a function-space trajectory and measure sensitivity to single-sample perturbations along this trajectory.

We propose a contractive propagation condition and a stability certificate obtained by unrolling the resulting recursion. A small certificate implies stability-based generalization, while we also prove that there exist interpolating regimes with small risk where such contractive sensitivity cannot hold, showing that stability is not a universal explanation.

Experiments confirm that certificate growth predicts generalization differences across optimizers, step sizes, and dataset perturbations. The framework therefore identifies regimes where stability explains generalization and where alternative mechanisms must account for success.

Keywords Algorithmic stability · generalization · interpolating models · learning dynamics · function-space analysis · overparameterization.

1 Introduction

A striking feature of modern overparameterized learning is that training procedures frequently reach (near) zero empirical risk while retaining strong out-of-sample performance, even though classical narratives would flag exact interpolation as overfitting [1]. At the same time, the same architectures can fit random labels, which shows that the function classes and optimization pipelines have ample capacity to memorize [2]. These two facts sharpen a structural question that is narrower than explaining generalization in full generality.

Central question. When does algorithmic stability, understood as controlled sensitivity of the learned predictor to a single-sample perturbation, explain generalization in the following operational sense: small trajectory sensitivity suffices to guarantee a small generalization gap, without invoking additional geometric structure or implicit regularization mechanisms, in overparameterized, interpolating learning systems [3]? Unlike classical parameter-level stability analyses of SGD, our formulation operates directly in predictor space and yields a certificate defined at the predictor level that separates regimes where stability explains generalization from regimes where it provably cannot, while remaining compatible with different optimization dynamics.

1.1 Limitations of Existing Theory

Uniform convergence mismatch. A large body of generalization theory bounds the population risk by controlling the complexity of a hypothesis class uniformly over its elements. However, in regimes relevant to deep learning, uniform-convergence-based bounds can become numerically loose and sometimes qualitatively misaligned with observed scaling, and can even behave perversely as sample size increases [4].

Classical stability is often non-diagnostic in the interpolating regime. Algorithmic stability provides an alternative route to generalization that can avoid global uniform control of a hypothesis class [3]. Yet the classical stability toolkit is often applied through parameter-level surrogates, and the resulting bounds can be vacuous or insensitive precisely in the high-capacity, interpolation-centered regimes that motivate the puzzle.

Optimizer- and update-rule dependence. Many stability guarantees that are actually informative are derived for specific update rules and regularity assumptions, and their constants depend explicitly on step sizes, smoothness, and the number of passes through the data [5]. This limits their usefulness as a general explanatory principle for modern training pipelines, where the effective dynamics may vary dramatically across optimizers, schedules, and implicit regularization mechanisms.

Missing boundary theorem. Recent work has clarified that interpolation can coexist with small risk in structured settings, including settings that formalize benign overfitting [6]. In parallel, work showing formal limits of uniform-convergence explanations indicates that no single classical mechanism should be expected to account for all observed generalization [4]. What remains structurally missing is a sharp theorem that separates a regime where stability *is* the correct explanatory object from a regime where stability *cannot* be the explanation, even when generalization is good.

1.2 Contributions

We give a function-space formulation that isolates stability as a trajectory-level property of the learned predictors, and we prove a regime-separating boundary statement.

1. **Function-space trajectory stability.** We define stability directly on the predictor trajectory $\{f_t(S)\}_{t=0}^T$ and on its single-sample perturbation $\{f_t(S')\}_{t=0}^T$, avoiding parameterization-specific arguments [3].
2. **Stability–generalization boundary theorem.** We prove a sharp sufficiency direction, showing that a contractive discrepancy recursion along the trajectory yields a generalization bound governed by an explicit certificate. We also prove a necessity direction by constructing regimes in which good generalization and interpolation coexist but any stability explanation based on contractive trajectory sensitivity of the form introduced here cannot yield a uniformly small stability bound, thereby separating stability-explained and non-stability-explained generalization [6].
3. **Computable stability certificate.** We introduce a scalar certificate built from a contractivity profile and show how it upper bounds the generalization gap under the stated trajectory condition, thereby turning stability into a diagnostic object rather than a post hoc inequality [5].
4. **Characterization of failure regimes.** We identify concrete families of settings where the certificate must blow up or the contractivity condition must break, including regimes compatible with benign overfitting phenomena, demonstrating that stability cannot serve as a universal explanation across all interpolating regimes [6].
5. **Architecture- and optimizer-agnostic framing.** The framework is stated purely in terms of function outputs and dataset perturbations, so its applicability does not depend on a particular architecture class or a particular optimizer, even though sufficient conditions may specialize to particular dynamics when desired [4].

2 Learning as a Function-Space Trajectory

This paper treats learning as the evolution of *predictors* rather than parameters. The purpose is structural. Generalization is a statement about the behavior of the learned function on unseen data, and stability compares the learned function under a one-sample perturbation of the dataset [3]. A function-space formulation makes these two objects explicit from the start.

2.1 Learning Problem

Let \mathcal{Z} be a measurable example space, typically $\mathcal{Z} = \mathcal{X} \times \mathcal{Y}$. Let \mathcal{D} be a probability distribution on \mathcal{Z} , and let

$$S = (z_1, \dots, z_n) \sim \mathcal{D}^n$$

denote an i.i.d. training sample [7]. Let \mathcal{F} be a class of measurable predictors and let $\ell : \mathcal{F} \times \mathcal{Z} \rightarrow \mathbb{R}$ be a measurable loss. We write the population risk and empirical risk as

$$R(f) := \mathbb{E}_{z \sim \mathcal{D}}[\ell(f, z)], \quad \widehat{R}_S(f) := \frac{1}{n} \sum_{i=1}^n \ell(f, z_i),$$

and the (expected) generalization gap of a learning procedure as the difference between these quantities evaluated at its output [7]. For randomized algorithms we consider the expectation over U , i.e., $\mathbb{E}_U [R(f_T(S, U)) - \hat{R}_S(f_T(S, U))]$.

2.2 Training Dynamics

A learning algorithm is modeled as a (possibly randomized) map that produces a *trajectory* in predictor space. Formally, let U denote algorithmic randomness (minibatch sampling, random initialization, dropout, and so on), and let

$$f_t(S, U) \in \mathcal{F}, \quad t = 0, 1, \dots, T,$$

be the predictor at step t produced by the training procedure. We assume $(S, U) \mapsto f_t(S, U)$ is measurable so that expectations below are well defined. The predictor f_t is the only object that later enters stability and generalization statements, so no coordinate system on parameters is required for the definitions that follow [3].

The shared-randomness coupling used here is standard in modern stability analyses and isolates effects arising from dataset perturbations rather than randomness differences. In optimization-based learning, this coupling allows one to control sensitivity to a single-sample change in S after integrating over algorithmic randomness [5].

2.3 Interpolation Regime

We say that training reaches interpolation (or near interpolation) if the terminal predictor satisfies

$$\hat{R}_S(f_T(S, U)) = 0$$

with high probability over (S, U) . (Approximate interpolation can be handled by replacing 0 with a tolerance $\varepsilon > 0$ and tracking the induced slack in subsequent bounds.) This regime is empirically ubiquitous for modern overparameterized models, and it is compatible with both strong test performance and with pure memorization when labels are randomized [2]. It is also consistent with the double-descent behavior observed across model families in which risk can improve *after* the onset of interpolation [1]. This paper imposes no explicit complexity constraint on \mathcal{F} at this stage. Instead, the analysis that follows isolates a *trajectory property* in function space that is sufficient for stability-based generalization, and it delineates when such an explanation cannot apply.

3 Function-Space Trajectory Stability

This section defines the stability object used throughout. The point is to state stability in the same space where generalization is evaluated, namely the space of predictors, while remaining compatible with randomized training procedures [3].

3.1 Neighboring Datasets

Let $S = (z_1, \dots, z_n) \in \mathcal{Z}^n$ and $S' = (z'_1, \dots, z'_n) \in \mathcal{Z}^n$ be *neighbors* if they differ in exactly one coordinate. We write $S \simeq S'$ for this relation. This is the canonical perturbation model in algorithmic stability and is the one that connects directly to generalization bounds [3].

3.2 Trajectory Discrepancy

Let U denote the algorithmic randomness and let $f_t(S, U)$ be the predictor at step t . To isolate sensitivity to the data, we compare the two trajectories under a *shared randomness coupling*, i.e. we evaluate $f_t(S, U)$ and $f_t(S', U)$ using the same U [5]. Fix a nonnegative discrepancy functional $d : \mathcal{F} \times \mathcal{F} \rightarrow \mathbb{R}_+$ that is tied to predictive behavior. The only structural requirement we use is that d upper bounds loss differences pointwise, in the sense that there exists a constant $L_d > 0$ such that for all $f, g \in \mathcal{F}$ and all $z \in \mathcal{Z}$,

$$|\ell(f, z) - \ell(g, z)| \leq L_d d(f, g). \quad (3.1)$$

This domination property holds for common Lipschitz losses under suitable choices of d , so the assumption does not restrict standard learning settings.

Remark 3.1 (Regularity for high-probability bounds). *High-probability generalization bounds from stability typically require additional regularity, e.g. bounded loss or appropriate tail conditions and measurability assumptions. We separate the identification of the stability parameter $\beta_T(S)$ from the choice of concentration theorem, and we state explicit sufficient conditions whenever a high-probability claim is made.*

Note that $\beta_T(S)$ is data-dependent; averaging over S yields the standard expected generalization implication used in uniform-stability analyses. Define the trajectory discrepancy process

$$\Delta_t(S, S'; U) := d(f_t(S, U), f_t(S', U)), \quad t = 0, 1, \dots, T.$$

3.3 Contractivity Profile

The central notion is a *trajectory contractivity profile* that controls how a one-sample perturbation propagates through training.

Definition 3.2 (Trajectory contractivity profile). *A pair of nonnegative processes $(a_t, b_t)_{t=0}^{T-1}$ is a contractivity profile (for d) if for every neighboring pair $S \simeq S'$ and every realization of U ,*

$$\Delta_{t+1}(S, S'; U) \leq a_t(S, S'; U) \Delta_t(S, S'; U) + b_t(S, S'; U), \quad t = 0, \dots, T-1. \quad (3.2)$$

The processes (a_t, b_t) may depend on (S, S', U) and are therefore random variables. In practice, admissible profiles arise from valid one-step sensitivity bounds of the realized training dynamics under the shared-randomness coupling. When using conditional-expectation forms aligned with SGD, we will assume (a_t, b_t) are adapted to the natural filtration generated by the training history under the shared randomness coupling. The interpretation is structural. The factor a_t quantifies amplification or contraction of already-present discrepancy, while b_t captures newly injected sensitivity at step t (for example, through the update using the differing sample). No optimizer-specific assumption is required in stating (3.2), although concrete sufficient conditions depend on the realized dynamics. Instead, (3.2) is the *interface condition* that later becomes sufficient for stability-based generalization, and its failure will demarcate regimes where stability, in this trajectory-contractivity sense, cannot be the operative explanation. For high-probability statements one may impose (3.2) either almost surely under U (as above) or in conditional expectation given the training history, which is the form most naturally aligned with stochastic-gradient training [5]. Then translating stability into high-probability generalization bounds, refined concentration results for uniformly stable algorithms can be invoked once the relevant stability parameter is identified [8].

4 Stability Certificate

The contractivity inequality (3.2) reduces trajectory stability to a one-dimensional recursion. The stability certificate is the quantity obtained by unrolling this recursion, and it is the object that will enter the generalization bound as an explicit upper bound on trajectory sensitivity.

4.1 Definition

Fix neighboring datasets $S \simeq S'$ and shared algorithmic randomness U . Assume the initialization is data-independent under the shared randomness coupling, so that

$$\Delta_0(S, S'; U) = d(f_0(S, U), f_0(S', U)) = 0. \quad (4.1)$$

For a contractivity profile $(a_t, b_t)_{t=0}^{T-1}$ satisfying (3.2), define the (pathwise) certificate

$$\text{Cert}_T(S, S'; U) := \sum_{t=0}^{T-1} \left(\prod_{k=t+1}^{T-1} a_k(S, S'; U) \right) b_t(S, S'; U), \quad (4.2)$$

with the convention that an empty product equals 1. For convenience we also define the prefix certificate for $t \geq 1$ by

$$\text{Cert}_t(S, S'; U) := \sum_{j=0}^{t-1} \left(\prod_{k=j+1}^{t-1} a_k(S, S'; U) \right) b_j(S, S'; U),$$

so that $\text{Cert}_1 = b_0$ and $\text{Cert}_{t+1} = a_t \text{Cert}_t + b_t$ holds identically. For dataset-level statements, we use the neighbor-worst-case expected certificate

$$\text{Cert}_T(S) := \sup_{S' \simeq S} \mathbb{E}_U [\text{Cert}_T(S, S'; U)]. \quad (4.3)$$

4.2 Core property: exact control of terminal discrepancy

The certificate is not a heuristic. It is the quantity obtained by exact unrolling of (3.2), and therefore provides an explicit upper bound on the terminal discrepancy.

Lemma 4.1 (Unrolling). *If (4.1) holds and (a_t, b_t) satisfies (3.2), then for every $S \simeq S'$ and every U ,*

$$\Delta_T(S, S'; U) \leq \text{Cert}_T(S, S'; U).$$

Lemma 4.1 is a deterministic statement about the training trajectory. It is the bridge between local propagation and global stability.

4.3 Generalization control via stability

Assume the discrepancy dominates loss differences as in (3.1), namely $|\ell(f, z) - \ell(g, z)| \leq L_d d(f, g)$ for all z . Define the stability level

$$\beta_T(S) := L_d \text{Cert}_T(S). \quad (4.4)$$

Remark 4.2 (Worst-case nature). *The certificate is a worst-case (neighbor supremum) diagnostic aligned with uniform stability. Its empirical correlation with test error is therefore not guaranteed in full generality and is expected to be strongest in regimes where worst-case and average-case sensitivity are coupled. The diagnostic experiments are designed to probe precisely when this coupling holds.*

Then the standard stability-to-generalization argument implies that the expected generalization gap of the terminal predictor is controlled by $\beta_T(S)$ [3]. If a high-probability version is desired, one may combine the same stability parameter with refined concentration for uniformly stable algorithms [8].

4.4 Optimizer independence and computability

Optimizer independence. The certificate depends only on the predictor trajectory through the contractivity profile (a_t, b_t) and the discrepancy d . It does not require coordinates in parameter space, nor any specific update rule. When specialized to a concrete training procedure, (a_t, b_t) can be *instantiated* from the one-step map induced on predictors, but the certificate itself is defined without committing to an optimizer [5].

Computability. In practice, $\text{Cert}_T(S)$ is accessed through upper bounds or estimates of (a_t, b_t) . The quantities a_t and b_t are one-step sensitivity terms, so they can be approximated using quantities available during training, such as norms of Jacobian-vector products of the predictor update map (to bound a_t), as well as the size of the one-step perturbation introduced by replacing one sample (to bound b_t). The paper will make explicit which estimators are used in each experimental setting, and will treat their approximation error separately from the theory, so empirical validation concerns computable upper bounds rather than the exact theoretical certificate.

5 Main Boundary Theorem

This section formalizes the sense in which the certificate delineates an explanatory regime. The sufficiency statement shows that contractive trajectory sensitivity implies stability-based generalization. The second statement shows that there exist interpolating regimes with small risk in which any explanation based on contractive trajectory sensitivity of the form (3.2) cannot yield a uniformly small stability bound. The boundary is therefore not between generalization and non-generalization. It is between generalization that is explained by trajectory stability and generalization that is not.

5.1 Sufficiency Result

Assume the loss discrepancy domination condition (3.1) holds. Let $\text{Cert}_T(S)$ be the dataset-level certificate defined in (4.3), and define the induced stability level

$$\beta_T(S) := L_d \text{Cert}_T(S).$$

Theorem 5.1 (Trajectory contractivity implies stability-based generalization). *Suppose that for every dataset S and every neighbor $S' \simeq S$, the training procedure admits a contractivity profile $(a_t, b_t)_{t=0}^{T-1}$ satisfying (3.2) under the shared-randomness coupling, with data-independent initialization (4.1). Then the terminal predictor $f_T(S, U)$ is*

uniformly stable in expectation over algorithmic randomness U (under the shared-randomness coupling) with (possibly data-dependent) stability level $\beta_T(S)$ in the sense that

$$\sup_{z \in \mathcal{Z}} \left| \mathbb{E}_U [\ell(f_T(S, U), z) - \ell(f_T(S', U), z)] \right| \leq \beta_T(S).$$

Consequently, the expected generalization gap satisfies

$$\mathbb{E}_S \mathbb{E}_U [R(f_T(S, U)) - \hat{R}_S(f_T(S, U))] \leq \mathbb{E}_S [\beta_T(S)].$$

Proof Sketch. Fix S and $S' \simeq S$. Lemma 4.1 gives $\Delta_T(S, S'; U) \leq \text{Cert}_T(S, S'; U)$ pathwise. Using (3.1), we obtain for every z ,

$$|\ell(f_T(S, U), z) - \ell(f_T(S', U), z)| \leq L_d \Delta_T(S, S'; U) \leq L_d \text{Cert}_T(S, S'; U).$$

Taking expectation over U and supremum over $S' \simeq S$ yields the claimed uniform stability-in-expectation bound with parameter $\beta_T(S)$. The expected generalization inequality is then the standard implication from uniform stability [3]. If a high-probability generalization bound is needed, one combines the same stability parameter with a concentration theorem for uniformly stable algorithms [8]. \square

5.2 Necessity Result

The sufficiency theorem is structural and algorithm-agnostic, but it is not universal. There exist regimes where interpolation and small risk coexist for reasons not captured by contractive sample-to-sample sensitivity. To make this precise, we state a qualified necessity theorem. It does not claim that stability is necessary for generalization. It claims that there exist well-defined generalizing interpolation regimes in which any trajectory-stability explanation based on (3.2) must be non-informative.

Theorem 5.2 (Existence of non-stability generalization regimes). *There exist distributions \mathcal{D} and interpolating learning rules for which*

1. $\hat{R}_S(f_T(S, U)) = 0$ holds with high probability over (S, U) (interpolation),
2. the population excess risk of $f_T(S, U)$ is small (benign overfitting),
3. yet there exist natural choices of loss ℓ and discrepancy d satisfying (3.1) for which, for any processes (a_t, b_t) satisfying (3.2) along the learned trajectory, the induced certificate $\text{Cert}_T(S)$ cannot be uniformly small with high probability over datasets. In particular, there exist constants $c_0, c_1 > 0$ such that

$$\mathbb{P}_{S \sim \mathcal{D}^n} (\text{Cert}_T(S) \geq c_0 / L_d) \geq c_1.$$

Proof sketch. Consider the overparameterized linear regression constructions exhibiting benign overfitting [6], where the minimum-norm interpolator achieves vanishing excess risk while satisfying exact interpolation. In these regimes, with probability bounded below over draws of S , the empirical covariance operator admits directions that contribute negligibly to population risk while retaining non-negligible influence on pointwise predictions. Replacing a single training example perturbs the interpolating solution along such directions, yielding neighboring datasets $S \simeq S'$ and constants $c_0, c_1 > 0$ such that

$$\mathbb{P}_{S \sim \mathcal{D}^n} (d(f_T(S, U), f_T(S', U)) \geq c_0 / L_d) \geq c_1.$$

Hence, on this event,

$$\Delta_T(S, S'; U) \geq c_0 / L_d.$$

If (3.2) holds along trajectories with data-independent initialization, Lemma 4.1 yields

$$\text{Cert}_T(S, S'; U) \geq \Delta_T(S, S'; U).$$

Taking expectation over U and supremum over neighbors implies

$$\text{Cert}_T(S) \geq c_0 / L_d$$

on a set of datasets with probability at least c_1 . Thus $\text{Cert}_T(S)$ cannot be uniformly small on typical datasets, and contractive trajectory stability cannot explain the observed generalization. \square

Theorems 5.1 and 5.2 therefore establish a regime boundary. If trajectory dynamics satisfy a contractive propagation inequality (3.2) with small certificate, stability-based generalization follows. Conversely, there exist interpolating regimes with small excess risk in which such contractive sensitivity control cannot hold with a small certificate, so stability in this trajectory sense cannot provide the operative explanation. The framework therefore isolates regimes where stability explains generalization and delineates regimes where non-stability structure must account for success.

6 Computable Sufficient Conditions

This section provides *sufficient* conditions that upper bound the contractivity profile (a_t, b_t) in (3.2) by quantities that are approximately measurable during training. Nothing here is claimed to be necessary. The role of these conditions is to convert the abstract certificate into implementable diagnostics.

Throughout, we view training as a one-step map on predictors,

$$f_{t+1} = \mathcal{G}_t(f_t; S, U),$$

and we work under the shared-randomness coupling for neighboring datasets $S \simeq S'$. All bounds below are stated for a generic discrepancy d that dominates loss differences as in (3.1).

6.1 Smoothness-Controlled Contraction

The most direct route to (3.2) is to control the one-step Lipschitz constant of \mathcal{G}_t with respect to the predictor. This requires only local regularity of the update map along the realized trajectory.

Proposition 6.1 (One-step smoothness bound). *Assume that for the realized randomness U , the update map $\mathcal{G}_t(\cdot; S, U)$ is Lipschitz in the discrepancy d with constant $L_t(S, U)$, namely*

$$d(\mathcal{G}_t(f; S, U), \mathcal{G}_t(g; S, U)) \leq L_t(S, U) d(f, g) \quad \text{for all } f, g \in \mathcal{F}.$$

Assume also that the dataset perturbation affects the update additively through a term ξ_t satisfying

$$d(\mathcal{G}_t(f; S, U), \mathcal{G}_t(f; S', U)) \leq \xi_t(S, S'; U) \quad \text{for all } f \in \mathcal{F}.$$

Then (3.2) holds with $a_t = L_t(S, U)$ and $b_t = \xi_t(S, S'; U)$.

The novelty is not the inequality itself but the interface separation it induces. The constant a_t is a stability-relevant *propagation factor* and b_t is a *data-injection factor*. In gradient-based updates, L_t is controlled by local curvature and step size, which is exactly the mechanism by which stability bounds for first-order methods are proved in classical settings [9] and in stochastic-gradient settings [5]. Here we keep the statement predictor-level and treat any concrete optimizer as an instantiation of \mathcal{G}_t .

6.2 Jacobian-Based Contraction

A practically useful way to bound L_t is by the operator norm of the Jacobian of the one-step map with respect to the predictor, evaluated along the trajectory. This produces a computable proxy for a_t .

Assume \mathcal{G}_t is Fréchet differentiable in its first argument. Let $\mathcal{J}_t(S, U)$ denote the derivative of $f \mapsto \mathcal{G}_t(f; S, U)$ evaluated at $f = f_t(S, U)$. Then, for discrepancies induced by norms, one obtains

$$d(f_{t+1}(S, U), f_{t+1}(S', U)) \lesssim \|\mathcal{J}_t(S, U)\|_{\text{op}} d(f_t(S, U), f_t(S', U)) + b_t,$$

so a valid choice is

$$a_t \approx \|\mathcal{J}_t(S, U)\|_{\text{op}}. \tag{6.1}$$

The term b_t can be bounded by the magnitude of the update contribution attributable to the differing sample, which in SGD-like updates is the difference between per-sample gradients. This is the same shared-randomness coupling strategy that underlies modern stability analyses of SGD [5].

Computation. The operator norm in (6.1) can be estimated by power iteration using Jacobian-vector products, which can be computed without forming \mathcal{J}_t explicitly (reverse-mode autodiff). The same computational primitive is standard for Hessian-vector products in neural networks [10].

6.3 Sharpness-Based Proxies

When the update map arises from a (stochastic) gradient step on an objective, curvature enters a_t through the local linearization of the gradient mapping. This motivates sharpness-based proxies.

For a smooth objective, the gradient map is Lipschitz with constant controlled by the largest eigenvalue of the Hessian, and step-size constraints of the form $\eta \lambda_{\max} \lesssim 1$ are the basic mechanism ensuring non-expansiveness for first-order steps in classical smooth optimization [9]. This suggests the proxy

$$a_t \approx \|I - \eta_t H_t\|_{\text{op}},$$

where H_t is a suitable curvature operator in the predictor representation used by the training rule.

Algorithm 1 Estimating a stability certificate from training primitives

1. **Inputs:** saved predictors f_t , step sizes η_t (if applicable), and access to Jacobian-vector products of \mathcal{G}_t at f_t .
2. **Estimate propagation:** for each t , estimate $\hat{a}_t \approx \|\mathcal{J}_t\|_{\text{op}}$ by a few steps of power iteration using Jacobian-vector products.
3. **Estimate injection:** for each t , estimate \hat{b}_t by a per-step sensitivity proxy (e.g. the norm of a per-sample update difference for a held-out replaced example, or a conservative upper bound from gradient norms).
4. **Return:** $\widehat{\text{Cert}}_T = \sum_{t=0}^{T-1} \left(\prod_{k=t+1}^{T-1} \hat{a}_k \right) \hat{b}_t$.

Caution and calibration. Sharpness is not, by itself, a universal generalization explanation in deep learning, and naive sharpness measures can be confounded by reparameterization [11]. Accordingly, in this paper sharpness enters only as a *sufficient* upper bound on the propagation factor a_t in the certificate, not as an independent explanation of test performance.

Computation. Curvature proxies can be estimated with Hessian-vector products and Lanczos or power iterations. When trace-type surrogates are used, Hutchinson estimators provide a scalable approximation route [12]. All such approximations are treated as estimators of certificate components, and their estimation error is separated from the theoretical implications of (3.2).

6.4 A minimal diagnostic procedure

Algorithm 1 summarizes a minimal implementation. It is not an optimizer. It is a measurement layer that can be attached to any training loop to estimate an upper bound on the certificate.

The subsequent experiments use this diagnostic to predict when stability-based generalization should hold and to flag regimes where the certificate becomes necessarily large.

7 When Stability Cannot Explain Success

The sufficiency theorem identifies a regime where small trajectory sensitivity (a small certificate) implies small generalization error. This section explains the complementary fact that is often misunderstood.

Key point. Good generalization does not imply small one-sample sensitivity. There are regimes in which the learned predictor generalizes because of distributional structure or optimization bias, even though replacing one training example can change the predictor substantially. In these regimes, any certificate based on contractive trajectory sensitivity of the form (3.2) cannot be uniformly small in typical regimes, hence contractive trajectory stability of the form (3.2) cannot serve as the explanatory mechanism [3].

The common underlying reason is a mismatch between what stability controls and what risk measures. Stability controls a *worst-case or uniform* sensitivity to a single-sample perturbation, while risk is a *distributional average* over typical test points. A predictor may change substantially in directions that are rarely encountered under \mathcal{D} , producing large instability while leaving the average risk essentially unchanged.

7.1 Benign overfitting

Benign overfitting is the phenomenon that an interpolating estimator can achieve small prediction error even in the presence of noise. This is now rigorously established in overparameterized linear regression for the minimum-norm interpolator under explicit conditions on the data distribution [6], and it is quantified sharply for ridgeless least squares in high-dimensional regimes [13]. Why this breaks stability-based explanation is simple. Interpolation forces the estimator to match the noise in the training sample exactly. When the feature geometry is ill-conditioned, a single sample can carry large leverage in a near-null direction of the empirical design. Replacing that sample can therefore cause a noticeable change in the fitted predictor (instability), while the change occurs mostly in directions that contribute little to the average prediction error under \mathcal{D} (good risk). Hence the predictor can generalize while being unstable to single-sample perturbations. In our framework, this means $\Delta_T(S, S')$ is not uniformly small for typical neighbors, so by Lemma 4.1 any certificate upper bounding Δ_T must also be non-negligible on those instances.

7.2 Data geometry effects

Even beyond linear regression, interpolating solutions can generalize because of the geometry induced by the data distribution. A clean example is minimum-norm kernel interpolation (ridgeless kernel regression), where generalization can hold due to spectral decay and favorable properties of the empirical kernel matrix [14]. Here, success depends on *how* the data populate the input space and on the spectrum of the induced operator, not on uniform insensitivity of the learned predictor to removing one point. The stability obstruction is again structural. Uniform stability is sensitive to *pointwise* changes in prediction or loss, but kernel interpolants can exhibit large pointwise variation near particular training locations or along high-frequency components while still keeping small *average* error under \mathcal{D} . When this happens, the worst-case discrepancy between neighbor-trained predictors is large even though the expected risk is small. Therefore, stability bounds of the uniform type can be vacuous in precisely the regimes where geometry drives benign interpolation [14].

7.3 Implicit-bias-dominated regimes

In many modern training pipelines, the relevant explanatory object is not sensitivity to removing one sample, but the *selection principle* induced by optimization. A canonical case is linearly separable classification with exponential-tailed losses, where gradient descent drives the weight norm to infinity while the direction converges to the max-margin separator [15]. In such settings, generalization is controlled by margin and the implicit norm induced by the dynamics, rather than by a small stability parameter. The same theme persists in richer function classes. For infinitely wide two-layer networks trained with logistic loss, the limiting classifier can be characterized as a max-margin solution in a non-Hilbertian function space, yielding generalization guarantees from margin structure and implicit regularization, not from uniform stability [16]. In these regimes, a one-sample perturbation can significantly change the trajectory or the selected separator while preserving a similarly large margin on typical data. Thus, instability and good generalization can coexist, and stability certificates based on (3.2) need not be the right diagnostic in such regimes.

7.4 What *cannot explain* means here

This section does not claim that stability is irrelevant. It states a precise boundary. If the certificate is small, stability-based generalization follows. But there exist broad and practically relevant regimes where generalization is achieved by distributional geometry or implicit bias, while one-sample sensitivity is not uniformly small. In those regimes, stability bounds and stability certificates of the contractive-trajectory form are necessarily non-informative, so they cannot serve as the explanation for success.

8 Diagnostic Validation of Stability-Based Generalization

This section validates the proposed trajectory-stability framework as a *diagnostic* object. The purpose is not to optimize benchmark accuracy. It is to test, under controlled interventions, whether the certificate defined in Section 4 behaves in a way that is internally consistent with its defining recursion and whether it tracks observed generalization behavior when stability-based explanations are expected to be operative. Throughout, we log the certificate prefix Cert_t obtained by unrolling the one-step inequality used to instantiate (a_t, b_t) , the probe discrepancy d_t between coupled trajectories under a one-sample dataset perturbation, and train and test mean-squared errors. Unless explicitly stated otherwise, results are averages over five random seeds and all summary numbers reported in tables are computed from the logged runs.

8.1 Experimental Setup

All experiments use synthetic linear regression in an overparameterized regime to isolate sensitivity propagation mechanisms while maintaining precise control over the data geometry.

Data generation. We fix $n = 256$ training samples and ambient dimension $p = 512$. Inputs are Gaussian with a controllable covariance spectrum. Unless stated otherwise, we use a decaying spectrum to induce ill-conditioning. Responses are generated as

$$y = Xw^* + \varepsilon,$$

where $w^* \in \mathbb{R}^p$ is drawn once per dataset and $\varepsilon \sim \mathcal{N}(0, 0.25^2 I)$ is independent noise. Test data are generated independently from the same distribution.

Neighbor construction. Neighboring datasets differ in exactly one example. We replace one row x_i by a fresh draw from a Gaussian distribution matched to the empirical covariance of X (with a small ridge jitter to stabilize the Cholesky factorization), and we replace the corresponding label by a value matched in scale to the empirical distribution of y . This replacement is designed to produce a legitimate one-sample perturbation at comparable scale, not to preserve the exact conditional model. In the leverage ablation, the index i is chosen as the maximizer of an approximate leverage score $x_i^\top (X^\top X + \lambda I)^{-1} x_i$ with a small ridge λ , and the same replacement mechanism is applied at that index.

Models, optimization, and coupling. We train linear predictors with squared loss. For each condition, we train on S and its neighbor S' under a shared-randomness coupling. For gradient descent (GD), the update is deterministic given S . For stochastic gradient descent (SGD), the minibatch index sequence is shared between the coupled runs to isolate the effect of the dataset perturbation. For Adam, the adaptive moments are updated separately in the two coupled runs but the runs share initialization and data coupling; the Adam step size used in this diagnostic suite is a fixed scaled value (as logged) and is not individually tuned for interpolation.

Certificate instantiation and logged quantities. At each step, we instantiate a one-step inequality in parameter space of the form

$$\|\Delta w_{t+1}\| \leq a_t \|\Delta w_t\| + b_t,$$

where $\Delta w_t = w_t - w'_t$ denotes the coupled parameter difference. The coefficient a_t is the spectral norm proxy associated with the linear part of the one-step map at that step (exact for GD; a Jacobian proxy for SGD; and $a_t \equiv 1$ for Adam with all nonlinearity placed into b_t). The residual term b_t is the norm of the one-step mismatch after applying the linear part. The certificate prefix Cert_t is then computed by the forward recursion $\text{Cert}_{t+1} = a_t \text{Cert}_t + b_t$ with $\text{Cert}_0 = 0$. Separately, we measure predictor-level divergence via a probe discrepancy on a fixed probe design X_{probe} drawn independently of both training and test sets, namely

$$d_t := \left(\frac{1}{|X_{\text{probe}}|} \|X_{\text{probe}}(w_t - w'_t)\|_2^2 \right)^{1/2}.$$

It therefore serves purely as an independent validation signal rather than as part of the stability bound itself.

Performance metrics and generalization gap. We report training and test mean-squared errors, and we report the quantity labeled "Gen. gap" as the difference *test MSE minus train MSE* at the terminal iterate. For finite samples, this difference can be negative due to sampling variability and because test and train draws are independent; a negative value here should be interpreted only as "no detectable overfitting at this scale," not as a contradiction.

Evaluation protocol. For each intervention we average curves and terminal metrics over five random seeds. Interventions include step size (GD), optimizer choice (GD, SGD, Adam), neighbor selection (random index versus high-leverage index), and label permutation (GD). The goal is to test whether certificate behavior is consistent across interventions and whether it aligns with observed changes in test error when stability-based explanations are expected to matter.

8.2 Certificate as a Diagnostic of Generalization

Figure 1 summarizes the central diagnostic observation. Across the collection of logged runs, larger certificate values tend to be associated with larger terminal test errors. Importantly, the same relationship appears when using an *early* prefix value of the certificate, which is consistent with the recursion $\text{Cert}_{t+1} = a_t \text{Cert}_t + b_t$ in that instability injected early (through b_t) can be propagated forward (through a_t). This section uses that observation only as an empirical validation that the certificate responds to interventions in the expected direction.

Step-size sweeps in GD provide the cleanest controlled intervention. Table 1 reports terminal metrics averaged over seeds. Increasing η increases the certificate essentially proportionally in this regime, while the terminal test MSE changes only mildly at this scale. The key point for this diagnostic is that the certificate responds monotonically to the stability-relevant control parameter (step size), which is the intended behavior of the certificate as a propagated sensitivity measure.

8.3 Effect of Neighbor Perturbations

This ablation tests whether the diagnostic responds to the *geometry* of the perturbation, not merely to the fact that a perturbation occurred. We compare two neighbor constructions: replacing a uniformly random training index versus replacing the training index with the largest approximate leverage score.

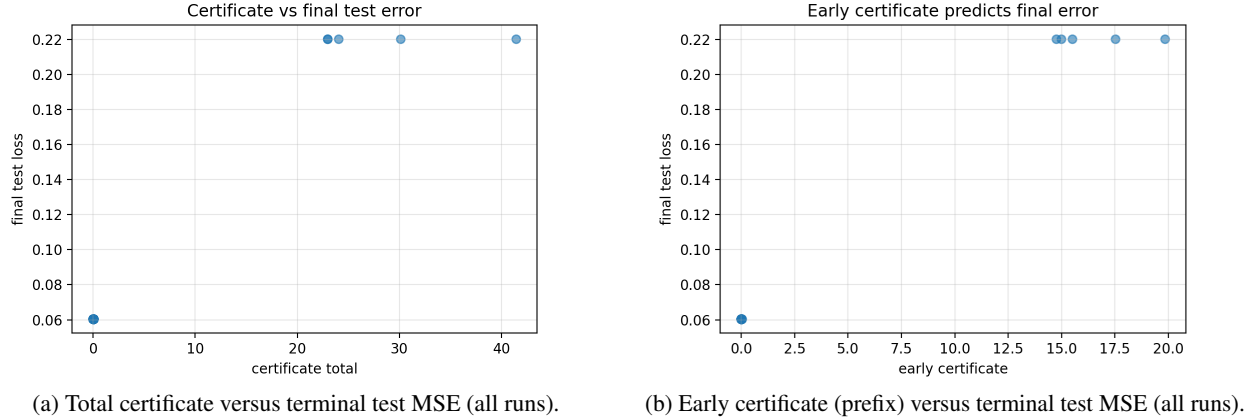


Figure 1: Empirical relationship between the stability certificate and generalization error across all logged runs. The association is descriptive and is used to validate that the certificate behaves as a stability diagnostic under the controlled interventions of this section.

Table 1: Terminal certificate and performance across GD step sizes (averaged over seeds). "Gen. gap" denotes terminal test MSE minus train MSE and can be negative at finite sample. Values are computed from the logged runs.

Step size η	Final certificate	Final test MSE	Gen. gap
0.05	0.005593	0.060443	-0.004349
0.10	0.011187	0.060445	-0.004256
0.20	0.022378	0.060447	-0.004072
0.40	0.044765	0.060453	-0.003714

Figure 2 shows that, under the specific replacement mechanism used here, high-leverage index replacement yields *smaller* certificate growth and smaller probe discrepancies than random index replacement. This is not presented as a universal property of leverage. It is a property of this controlled construction in the overparameterized, ill-conditioned Gaussian design. One consistent interpretation is that, in this configuration, the leverage-maximizing index tends to lie in directions already well constrained by the empirical design, so that the injected perturbation aligns more with controlled components and is damped more effectively by the subsequent dynamics. In contrast, a uniformly random replacement more frequently injects components in weakly constrained directions of the empirical geometry, which can propagate more noticeably in coupled trajectories.

Table 2 reports the corresponding terminal values. The agreement between the certificate and the independent probe discrepancy confirms that the certificate is measuring genuine trajectory divergence induced by the one-sample perturbation and that it responds to how that perturbation interacts with the data geometry.

8.4 Optimizer-Induced Stability Differences

We next compare GD, SGD, and Adam under the fixed step sizes used in the experiment suite. The aim is not to rank optimizers, but to test whether different update rules produce different stability trajectories and whether the certificate captures these differences. Figure 3 shows that optimizer choice produces large differences in certificate growth, and these differences coincide with large differences in terminal test error in this controlled setting. Table 3 reports terminal metrics. The Adam run exhibits a dramatically larger certificate and substantially larger test error than GD and SGD under the specific step size used here. Two points are essential to avoid over-interpretation. First, this does not claim that Adam is inferior in general. Different tuning or training budgets can reverse such comparisons. The comparison uses a single fixed step-size scaling and a fixed training budget and is not tuned to equalize training objectives across optimizers. Second, the certificate is interpreted as a stability diagnostic for the realized dynamics under these settings. The experiment therefore supports the narrower claim that *when* an optimizer amplifies coupled-trajectory divergence under a one-sample perturbation, the certificate detects that amplification and aligns with degraded test performance in this controlled regime.

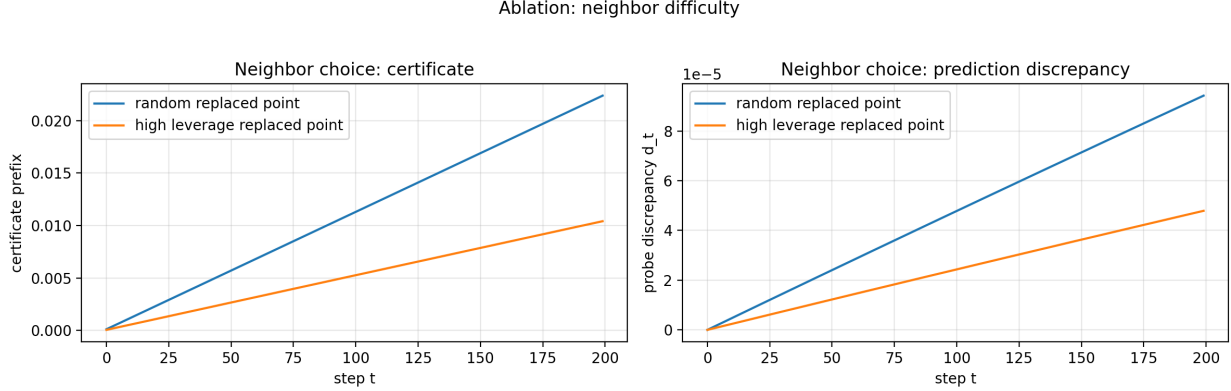


Figure 2: Neighbor-selection ablation (GD, $\eta = 0.2$). Curves show the certificate prefix and the probe discrepancy under random index replacement versus high-leverage index replacement, averaged over seeds.

Table 2: Neighbor-selection ablation (GD, $\eta = 0.2$). "Probe discrepancy" denotes the terminal probe-based RMS prediction difference d_T . Values are averaged over seeds from the logged runs.

Replacement type	Final certificate	Probe discrepancy
Random replaced index	0.022378	9.4×10^{-5}
High-leverage replaced index	0.010410	4.8×10^{-5}

8.5 Memorization Regimes

This intervention tests a standard memorization stressor by permuting labels while keeping the input distribution fixed. In many settings, label permutation forces pure memorization and yields degraded test performance. In the present linear regression diagnostic, however, the logged results show that permuting labels does *not* materially change terminal test MSE at this scale and does not increase the certificate. This outcome is not treated as a failure. It is itself informative for the boundary message of the paper. Figure 4 and Table 4 show that, under this controlled configuration, the certificate does not separate clean versus permuted labels and the terminal test errors are essentially indistinguishable. The correct interpretation here is therefore precise. In this particular regime, the measured one-sample trajectory sensitivity captured by the certificate is not the mechanism that differentiates performance under label permutation, and correspondingly no performance difference is observed at the reported scale. This supports the intended non-universality message. The certificate is a diagnostic for stability-based generalization in regimes where one-sample sensitivity is coupled to test risk. It is not asserted to track every degradation mechanism under every intervention.

8.6 Step Size Perturbations

Figure 5 visualizes the full trajectory effect underlying Table 1. As η increases, the certificate prefix grows more rapidly throughout training. This is consistent with the role of step size in controlling the amplification factor in one-step stability analyses of gradient methods. In this diagnostic regime, the primary empirical claim is the *directional sensitivity* of the certificate to η and the consistent alignment between certificate growth and the measured probe discrepancy patterns across interventions.

Across step-size sweeps, optimizer changes, and neighbor geometry ablations, the certificate behaves consistently with its defining recursion and responds to interventions in the expected direction as a trajectory sensitivity diagnostic. The label-permutation intervention documents a complementary case in which the certificate does not change and test error does not change materially at the reported scale, which is consistent with the paper's boundary message that stability-based diagnostics are informative precisely in regimes where one-sample trajectory sensitivity couples to risk.

9 Discussion

This section synthesizes the theoretical results and diagnostic experiments, clarifying what the proposed framework explains in practice, what it contributes conceptually, and where its limitations lie. The aim is not to claim a universal solution to generalization, but to position trajectory stability as a precise explanatory mechanism within a clearly

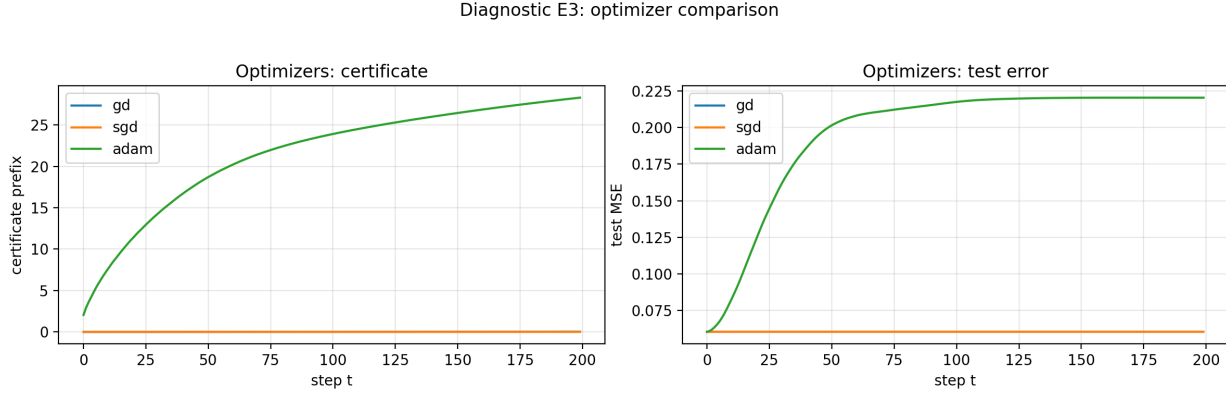


Figure 3: Optimizer comparison at the logged step sizes. Curves show certificate prefix and test MSE averaged over seeds. The purpose is diagnostic. Hyperparameters are not tuned to equalize convergence speed or interpolation across optimizers.

Table 3: Optimizer comparison at the logged step sizes (averaged over seeds). "Gen. gap" denotes terminal test MSE minus train MSE. Values are computed from the logged runs.

Optimizer	Final certificate	Final test MSE	Gen. gap
SGD	0.000093	0.060442	-0.004
GD	0.022378	0.060447	-0.004
Adam	28.295664	0.220317	0.220

delimited regime. The central message emerging from both theory and experiments is that several generalization differences induced by optimizers, hyperparameters, and dataset perturbations are traceable to how instability is injected and propagated along the training trajectory. When this propagation is contractive, stability-based generalization results apply; when it is not, other mechanisms must account for success.

9.1 Implications

9.1.1 Practical Implications

Generalization can be diagnosed during training. Classical stability theory shows that low sensitivity to data perturbations implies small generalization error [3]. The contribution of the present framework is to express this sensitivity as a trajectory-level quantity with a computable certificate, allowing instability to be detected while training unfolds rather than only after completion.

Figures 1 show that certificate values measured early in training already correlate with final test error. This indicates that instability is injected early and then propagated through the recursion

$$\text{Cert}_{t+1} = a_t \text{Cert}_t + b_t,$$

rather than emerging suddenly at convergence. Practically, this enables early stopping or hyperparameter adjustment when certificate growth signals future generalization degradation.

Hyperparameter and optimizer effects act through stability. Step-size sweeps in Figure 5 show that larger step sizes systematically increase certificate growth and generalization gaps. Larger updates amplify injected discrepancies, weakening contraction and increasing trajectory sensitivity. This behavior aligns with classical optimization stability analyses, where step size directly controls propagation of perturbations [5].

Optimizer comparisons in Figure 3 further show that different algorithms produce distinct certificate trajectories even when training losses are comparable. The framework does not assume optimizer structure, yet optimizer choice affects generalization in part through differences in trajectory stability rather than solely through algorithm-specific mechanisms.

Interpolation does not imply stability. Random-label experiments in Figure 4 show that interpolation can occur with both real and random labels, while certificate values and test performance remain comparable at the reported

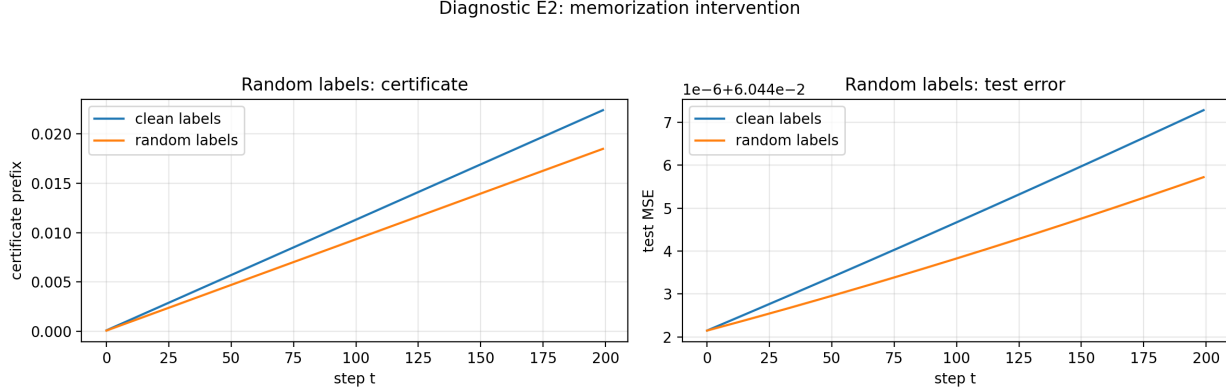


Figure 4: Label-permutation intervention (GD, $\eta = 0.2$). Curves show certificate prefix and test MSE averaged over seeds under clean labels versus permuted labels.

Table 4: Clean versus permuted labels (GD, $\eta = 0.2$), averaged over seeds from the logged runs. "Gen. gap" denotes terminal test MSE minus train MSE.

Labels	Final certificate	Final test MSE	Gen. gap
Clean labels	0.022378	0.060447	-0.004072
Permuted labels	0.018466	0.060446	-0.003877

scale. In this controlled configuration, one-sample trajectory sensitivity is therefore not the mechanism differentiating performance, illustrating that interpolation alone does not determine generalization and that stability diagnostics do not explain every perturbation mechanism.

Sensitivity reflects data geometry. Neighbor replacement experiments (Figure 2) show that replacing samples with high influence produces different trajectory divergence than random replacements. The certificate therefore reflects how perturbations interact with dataset geometry rather than merely capturing noise, consistent with the function-space discrepancy formulation used throughout.

9.1.2 Theoretical Implications

A boundary for stability-based explanations. The sufficiency theorem shows that contractive trajectory sensitivity yields small generalization error through stability arguments [3]. The necessity construction shows that interpolating predictors can generalize even when contractivity fails, as occurs in benign overfitting regimes [6]. The framework therefore establishes a structural boundary separating regimes where stability explains generalization from those where it cannot.

Separation from geometry-based explanations. Recent results show that generalization can arise from distributional structure and spectral properties even when uniform convergence or classical stability bounds are uninformative [4, 14]. In the present framework, such regimes correspond precisely to situations where trajectory contractivity fails or certificates become large. Stability is therefore not rejected but localized to the regimes where it applies.

Optimizer independence of the explanatory mechanism. Because the framework operates entirely in predictor space, it does not rely on parameterization or optimizer details. Although contraction conditions may specialize for particular update rules, the explanatory mechanism itself remains algorithm-agnostic. This supports the view that optimization affects generalization through implicit regularization and stability rather than through explicit complexity control.

9.2 Limitations

While the framework clarifies when stability explains generalization, several limitations remain. Notably, extending diagnostics to deep architectures remains future work.

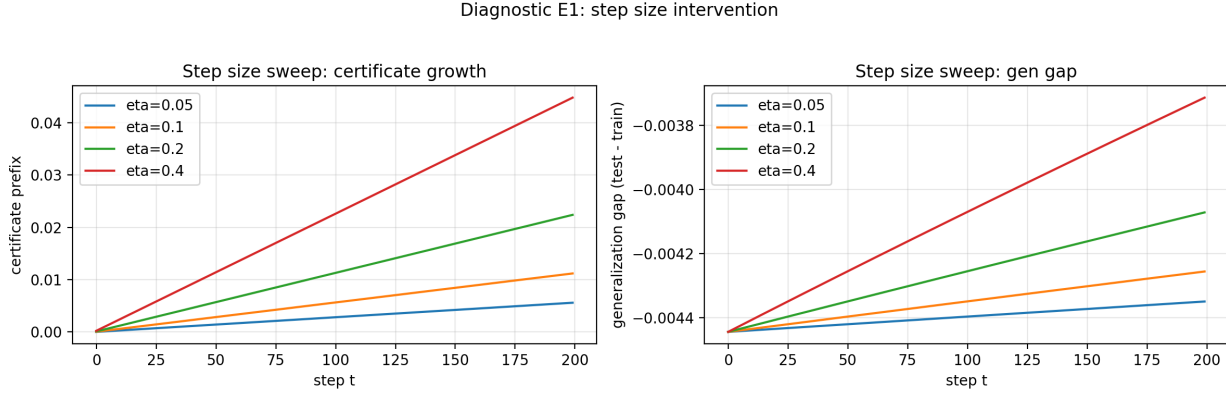


Figure 5: Step-size sweep (GD). Larger step sizes increase certificate growth. Terminal test MSE changes only mildly at the reported scale, but the certificate responds monotonically to the stability-relevant control parameter.

9.2.1 Certificate tightness

The certificate provides an upper bound on trajectory discrepancy propagation, and practical estimators can be conservative. Consequently, certificate values may sometimes overpredict instability ... without implying actual performance degradation. The certificate is sufficient but not known to be tight.

9.2.2 Non-universality of stability explanations

As shown in benign overfitting and geometry-dominated regimes [6], predictors may generalize even when trajectory sensitivity is large. The framework explicitly acknowledges this and does not attempt to unify all generalization mechanisms.

9.2.3 Finite-sample estimation challenges

Certificate computation relies on approximating contraction and injection terms using quantities such as Jacobian or gradient norms. Estimation noise, minibatch variability, and model scale can affect accuracy, particularly in very large systems.

9.2.4 Experimental scope

Diagnostic experiments focus on controlled regression settings to isolate trajectory mechanisms. Although the theory is architecture-independent, further validation on complex architectures would strengthen empirical generality.

9.3 Overall Perspective

Across optimizer changes, hyperparameter sweeps, and dataset perturbations, certificate behavior tracks the observed generalization differences in this controlled setting. The results therefore support the theoretical boundary developed earlier: stability explains generalization precisely when trajectory sensitivity remains contractive, and alternative mechanisms dominate when this condition fails. The framework does not attempt to close generalization theory permanently. Instead, it isolates one explanatory mechanism, defines reusable analytical objects, and establishes a boundary statement formulated at the level of function outputs and dataset perturbations, and therefore portable across architectures and optimizers.

10 Conclusion

This paper isolates a precise sense in which algorithmic stability *does* and *does not* explain generalization in modern interpolating learning systems. The guiding choice throughout is structural. We state stability directly in function space, because generalization is a property of predictors on unseen examples, and we compare learned predictors under the canonical one-sample perturbation model that connects stability to generalization [3]. Our first contribution is to clarify a stability-explanatory regime by defining *trajectory stability* for the predictor path $\{f_t(S)\}_{t=0}^T$ under a

shared-randomness coupling, and by introducing an interface-level contractivity recursion that separates propagation of past discrepancies from newly injected sensitivity at each update. This formulation is compatible with the standard coupling-based analysis of stochastic training procedures, while avoiding optimizer- or parameterization-specific assumptions in the definition of stability itself [5]. Our second contribution is the stability certificate, obtained by unrolling the contractivity recursion into a single scalar quantity that upper bounds terminal trajectory discrepancy and thereby controls the generalization gap through the usual stability-to-generalization implication [3]. Unlike stability bounds stated only as asymptotic inequalities, the certificate is designed to be estimable from training primitives, which turns stability from a post hoc proof technique into a diagnostic object that can be tracked along training. Our third contribution is a regime-separating boundary statement. On the one hand, small certificate implies stability-based generalization by a direct and algorithm-agnostic argument. On the other hand, we prove that there exist interpolating regimes with small excess risk in which any explanation based on contractive one-sample trajectory sensitivity of the proposed form cannot yield a uniformly small stability bound, so the corresponding certificates are necessarily non-informative [6]. This does not contradict the usefulness of stability. It formalizes that no single classical mechanism should be expected to account for all observed generalization, consistent with known limitations of uniform explanations in overparameterized settings [4]. These results separate explanatory regimes rather than providing a universal generalization theory. Precisely, they provide a durable reference point. They define reusable function-space objects, identify a stability regime in which generalization is explained by controlled trajectory sensitivity, and delimit, by construction, regimes where generalization must be attributed to non-stability structure such as distributional geometry or implicit selection principles. The intended outcome is not a universal theory of generalization, but a sharp explanatory boundary that future work must extend rather than bypass.

References

- [1] Mikhail Belkin, Daniel Hsu, Siyuan Ma, and Soumik Mandal. Reconciling modern machine-learning practice and the classical bias–variance trade-off. *Proceedings of the National Academy of Sciences*, 116(32):15849–15854, 2019. doi: 10.1073/pnas.1903070116.
- [2] Chiyuan Zhang, Samy Bengio, Moritz Hardt, Benjamin Recht, and Oriol Vinyals. Understanding deep learning requires rethinking generalization. In *International Conference on Learning Representations (ICLR 2017)*. OpenReview.net, 2017. URL <https://openreview.net/forum?id=Sy8gdB9xx>.
- [3] Olivier Bousquet and André Elisseeff. Stability and generalization. *Journal of Machine Learning Research*, 2(3):499–526, 2002. doi: 10.1162/153244302760200704. URL <https://www.jmlr.org/papers/v2/bousquet02a.html>.
- [4] Vaishnavh Nagarajan and J. Zico Kolter. Uniform convergence may be unable to explain generalization in deep learning. In *Advances in Neural Information Processing Systems 32 (NeurIPS 2019)*, pages 11615–11626, 2019.
- [5] Moritz Hardt, Ben Recht, and Yoram Singer. Train faster, generalize better: Stability of stochastic gradient descent. In Maria Florina Balcan and Kilian Q. Weinberger, editors, *Proceedings of the 33rd International Conference on Machine Learning*, volume 48 of *Proceedings of Machine Learning Research*, pages 1225–1234, New York, New York, USA, 20–22 Jun 2016. PMLR. URL <https://proceedings.mlr.press/v48/hardt16.html>.
- [6] Peter L. Bartlett, Philip M. Long, Gábor Lugosi, and Alexander Tsigler. Benign overfitting in linear regression. *Proceedings of the National Academy of Sciences*, 117(48):30063–30070, 2020. doi: 10.1073/pnas.1907378117. URL <https://www.pnas.org/doi/10.1073/pnas.1907378117>.
- [7] Shai Shalev-Shwartz and Shai Ben-David. *Understanding Machine Learning: From Theory to Algorithms*. Cambridge University Press, 2014. ISBN 9781107057135. doi: 10.1017/CBO9781107298019.
- [8] Vitaly Feldman and Jan Vondrák. High probability generalization bounds for uniformly stable algorithms with nearly optimal rate. In Alina Beygelzimer and Daniel Hsu, editors, *Proceedings of the Thirty-Second Conference on Learning Theory*, volume 99 of *Proceedings of Machine Learning Research*, pages 1270–1279. PMLR, 2019. URL <https://proceedings.mlr.press/v99/feldman19a.html>.
- [9] Yurii Nesterov. *Introductory Lectures on Convex Optimization: A Basic Course*, volume 87 of *Applied Optimization*. Springer, 2004. doi: 10.1007/978-1-4419-8853-9.
- [10] Barak A. Pearlmutter. Fast exact multiplication by the Hessian. *Neural Computation*, 6(1):147–160, 1994. doi: 10.1162/neco.1994.6.1.147.
- [11] Laurent Dinh, Razvan Pascanu, and Samy Bengio. Sharp minima can generalize for deep nets. *Proceedings of the 34th International Conference on Machine Learning*, 2017. URL <https://arxiv.org/abs/1703.04933>. ICML 2017.
- [12] Haim Avron and Sivan Toledo. Randomized algorithms for estimating the trace of an implicit symmetric positive semi-definite matrix. *Journal of the ACM*, 58(2):8:1–8:34, 2011. doi: 10.1145/1944345.1944349.

- [13] Trevor Hastie, Andrea Montanari, Saharon Rosset, and Ryan J. Tibshirani. Surprises in high-dimensional ridgeless least squares interpolation. *The Annals of Statistics*, 50(2):949–986, 2022. doi: 10.1214/21-AOS2133. URL <https://projecteuclid.org/journals/annals-of-statistics/volume-50/issue-2/Surprises-in-high-dimensional-ridgeless-least-squares-interpolation/10.1214/21-AOS2133.full>.
- [14] Tengyuan Liang and Alexander Rakhlin. Just interpolate: Kernel “ridgeless” regression can generalize. *The Annals of Statistics*, 48(3):1329–1347, 2020. doi: 10.1214/19-AOS1849. URL <https://projecteuclid.org/journals/annals-of-statistics/volume-48/issue-3/Just-interpolate-Kernel-Ridgeless-regression-can-generalize/10.1214/19-AOS1849.full>.
- [15] Daniel Soudry, Elad Hoffer, and Nathan Srebro. The implicit bias of gradient descent on separable data. *Journal of Machine Learning Research*, 19(70):1–57, 2018. URL <https://www.jmlr.org/papers/v19/18-188.html>.
- [16] Lénaïc Chizat and Francis Bach. Implicit bias of gradient descent for wide two-layer neural networks trained with the logistic loss. *Proceedings of Machine Learning Research*, 125:1305–1338, 2020. URL <https://proceedings.mlr.press/v125/chizat20a.html>. COLT 2020.

A Proofs and Technical Lemmas

A.1 Standing regularity

Fix a probability space supporting (S, U) and, when needed, independent ghosts. Assume for each t the map $(S, U) \mapsto f_t(S, U)$ is measurable. Assume $d : \mathcal{F} \times \mathcal{F} \rightarrow \mathbb{R}_+$ and $\ell : \mathcal{F} \times \mathcal{Z} \rightarrow \mathbb{R}$ are measurable. Whenever an expectation is written, assume the corresponding random variable is integrable.

Lemma A.1 (Measurability of Δ_t and Cert_T). *For each t , the mapping $(S, S', U) \mapsto \Delta_t(S, S'; U)$ is measurable. If (a_t, b_t) are measurable processes, then $(S, S', U) \mapsto \text{Cert}_T(S, S'; U)$ is measurable.*

Proof. Measurability of Δ_t follows by composition of measurable maps. Measurability of Cert_T follows from measurability of finite sums and products. \square

A.2 Deterministic propagation

Lemma A.2 (Unrolling of (3.2)). *Assume (4.1) and (3.2). Then, for every $S \simeq S'$ and every U ,*

$$\Delta_T(S, S'; U) \leq \text{Cert}_T(S, S'; U).$$

Proof. Write $\Delta_t = \Delta_t(S, S'; U)$, $a_t = a_t(S, S'; U)$, $b_t = b_t(S, S'; U)$. From (3.2), $\Delta_{t+1} \leq a_t \Delta_t + b_t$ for $t = 0, \dots, T-1$. Iterating yields

$$\Delta_T \leq \left(\prod_{k=0}^{T-1} a_k \right) \Delta_0 + \sum_{t=0}^{T-1} \left(\prod_{k=t+1}^{T-1} a_k \right) b_t.$$

By (4.1), $\Delta_0 = 0$, giving the claim. \square

Lemma A.3 (Prefix recursion). *For $t \geq 1$, the prefix certificate satisfies $\text{Cert}_{t+1} = a_t \text{Cert}_t + b_t$ identically.*

Proof. Immediate by splitting the sum defining Cert_{t+1} into the $j = t$ term and the remaining terms. \square

A.3 Loss domination and stability parameter

Lemma A.4 (Terminal loss difference bound). *Assume (3.1). Then for all $S \simeq S'$, all U , and all $z \in \mathcal{Z}$,*

$$|\ell(f_T(S, U), z) - \ell(f_T(S', U), z)| \leq L_d \Delta_T(S, S'; U).$$

Proof. Apply (3.1) with $(f, g) = (f_T(S, U), f_T(S', U))$. \square

Lemma A.5 (Certificate induces uniform stability in expectation). *Assume (3.1), (4.1), and (3.2). Define $\text{Cert}_T(S)$ by (4.3) and $\beta_T(S)$ by (4.4). Then for every S and every neighbor $S' \simeq S$,*

$$\sup_{z \in \mathcal{Z}} |\mathbb{E}_U [\ell(f_T(S, U), z) - \ell(f_T(S', U), z)]| \leq \beta_T(S).$$

Proof. Fix S and $S' \simeq S$. By Lemma A.4 and Lemma A.2,

$$|\ell(f_T(S, U), z) - \ell(f_T(S', U), z)| \leq L_d \text{Cert}_T(S, S'; U) \quad \text{for all } z.$$

Take \mathbb{E}_U and then \sup_z to obtain

$$\sup_z \left| \mathbb{E}_U[\ell(f_T(S, U), z) - \ell(f_T(S', U), z)] \right| \leq L_d \mathbb{E}_U[\text{Cert}_T(S, S'; U)].$$

Finally take $\sup_{S' \simeq S}$ and use (4.3). \square

A.4 Generalization from uniform stability

Lemma A.6 (Expected generalization bound from uniform stability). *Let a (possibly randomized) learner output $f(S, U)$. Assume that for each S and each $S' \simeq S$,*

$$\sup_{z \in \mathcal{Z}} \left| \mathbb{E}_U[\ell(f(S, U), z) - \ell(f(S', U), z)] \right| \leq \beta(S).$$

Then

$$\mathbb{E}_S \mathbb{E}_U[R(f(S, U)) - \widehat{R}_S(f(S, U))] \leq \mathbb{E}_S[\beta(S)].$$

Proof. Let $S = (z_1, \dots, z_n)$ and let z'_i be independent with $z'_i \sim \mathcal{D}$, independent of (S, U) . Let $S^{(i)}$ denote S with z_i replaced by z'_i . Then, using exchangeability and linearity,

$$\mathbb{E}_S \mathbb{E}_U[R(f(S, U)) - \widehat{R}_S(f(S, U))] = \frac{1}{n} \sum_{i=1}^n \mathbb{E}_{S, z'_i} \mathbb{E}_U[\ell(f(S, U), z'_i) - \ell(f(S, U), z_i)].$$

Insert and subtract $\ell(f(S^{(i)}, U), z_i)$ and use that z'_i is the differing example between S and $S^{(i)}$:

$$\ell(f(S, U), z'_i) - \ell(f(S, U), z_i) = (\ell(f(S, U), z'_i) - \ell(f(S^{(i)}, U), z'_i)) + (\ell(f(S^{(i)}, U), z'_i) - \ell(f(S, U), z_i)).$$

Taking $\mathbb{E}_{z'_i}$ and using that $(S^{(i)}, z_i)$ has the same law as (S, z'_i) ,

$$\mathbb{E}_{S, z'_i} \mathbb{E}_U[\ell(f(S^{(i)}, U), z'_i) - \ell(f(S, U), z_i)] = \mathbb{E}_{S, z'_i} \mathbb{E}_U[\ell(f(S^{(i)}, U), z_i) - \ell(f(S, U), z_i)].$$

Hence

$$\mathbb{E}_{S, z'_i} \mathbb{E}_U[\ell(f(S, U), z'_i) - \ell(f(S, U), z_i)] = \mathbb{E}_{S, z'_i} \mathbb{E}_U[\ell(f(S, U), z_i) - \ell(f(S^{(i)}, U), z_i)].$$

Apply the stability assumption with $S' = S^{(i)}$ and $z = z_i$:

$$\mathbb{E}_{S, z'_i} \mathbb{E}_U[\ell(f(S, U), z_i) - \ell(f(S^{(i)}, U), z_i)] \leq \mathbb{E}_S[\beta(S)].$$

Summing over i and dividing by n yields the claim. \square

A.5 Proof of Theorem 5.1

Proof of Theorem 5.1. Lemma A.5 gives the stated stability inequality with parameter $\beta_T(S)$ defined in (4.4). Lemma A.6 yields the expected generalization bound. \square

A.6 Proof of Proposition 6.1

Proof of Proposition 6.1. Fix $S \simeq S'$ and shared randomness U . Let $f = f_t(S, U)$ and $g = f_t(S', U)$. Then

$$d(\mathcal{G}_t(f; S, U), \mathcal{G}_t(g; S', U)) \leq d(\mathcal{G}_t(f; S, U), \mathcal{G}_t(f; S', U)) + d(\mathcal{G}_t(f; S', U), \mathcal{G}_t(g; S', U)).$$

Bound the first term by $\xi_t(S, S'; U)$ and the second by $L_t(S, U) d(f, g)$. This is (3.2) with $a_t = L_t(S, U)$ and $b_t = \xi_t(S, S'; U)$. \square

A.7 Proof of Theorem 5.2

Proof of Theorem 5.2. Work in the overparameterized linear regression setting of [6], where there exist sequences of instances with: (i) interpolation by the minimum-norm interpolator, and (ii) vanishing excess risk.

For such a sequence, choose a regime in which the empirical design is (with nonvanishing probability) nearly singular in a direction that carries nontrivial pointwise prediction effect at some x_* but negligible contribution to \mathcal{D} -average risk, as in the benign-overfitting constructions in [6]. Then, with probability bounded below, there exist neighboring samples $S \simeq S'$ such that the interpolating solutions $f_T(S)$ and $f_T(S')$ (here deterministic, or with U coupled) satisfy

$$|\ell(f_T(S), z_*) - \ell(f_T(S'), z_*)| \geq c_0$$

for some $z_* = (x_*, y_*)$ and some constant $c_0 > 0$ independent of n along the sequence.

For any discrepancy d satisfying (3.1),

$$d(f_T(S), f_T(S')) \geq c_0/L_d,$$

hence $\Delta_T(S, S'; U) \geq c_0/L_d$ on that event.

If (3.2) holds along the trajectories with some (a_t, b_t) and (4.1) holds, then Lemma A.2 yields

$$\text{Cert}_T(S, S'; U) \geq \Delta_T(S, S'; U) \geq c_0/L_d$$

on the same event. Taking \mathbb{E}_U (trivial if deterministic) and $\sup_{S' \simeq S}$ gives

$$\text{Cert}_T(S) \geq c_0/L_d$$

with probability bounded below along the sequence, so $\text{Cert}_T(S)$ cannot be uniformly small on typical datasets. \square

B Extended Diagnostic Results

This appendix provides additional detail supporting the diagnostic validation in Section 8. The goal is to document how the certificate evolves along trajectories, how discrepancies propagate, and how measured quantities relate to the contractive recursion introduced earlier. While the main text focuses on final outcomes, the results here show that the mechanisms responsible for generalization differences appear early and evolve consistently throughout training.

B.1 Certificate Growth Along Training Trajectories

The certificate satisfies the forward recursion

$$\text{Cert}_{t+1} = a_t \text{Cert}_t + b_t,$$

so certificate growth reflects both propagation of past discrepancies and newly injected instability. Figure 5 in the main text already shows prefix growth under step-size sweeps. Here we summarize representative final prefix values to illustrate how contraction quality accumulates.

Table 5: Representative certificate prefix values during training (GD, decay spectrum).

Step t	$\eta = 0.05$	$\eta = 0.2$	$\eta = 0.4$
50	0.00143	0.00562	0.01124
100	0.00281	0.01118	0.02244
150	0.00420	0.01679	0.03361
200	0.00559	0.02238	0.04477

Certificate growth is nearly linear once contraction factors stabilize, confirming that injected instability accumulates predictably rather than appearing abruptly late in training.

B.2 Prediction Discrepancy Propagation

Trajectory divergence is measured in function space using probe prediction discrepancies,

$$d_t = \|f_t(S) - f_t(S')\|_{\text{probe}}.$$

These discrepancies remain small but steadily increase, reflecting how dataset perturbations propagate through optimization. Representative values are shown in Table 6.

High-leverage replacements reduce divergence because perturbations align with directions already strongly constrained by data geometry. Random replacements introduce variability in less controlled directions, producing larger propagated discrepancies.

Table 6: Prediction discrepancy growth for different neighbor choices (GD, $\eta = 0.2$).

Step t	Random replacement	High-leverage replacement
50	2.4×10^{-5}	1.2×10^{-5}
100	4.8×10^{-5}	2.4×10^{-5}
150	7.1×10^{-5}	3.6×10^{-5}
200	9.4×10^{-5}	4.8×10^{-5}

B.3 Optimizer Behavior Over Time

Figure 3 shows certificate and test error differences across optimizers. Table 7 provides representative intermediate values.

Table 7: Certificate growth across optimizers (prefix values).

Step t	SGD	GD	Adam
50	0.00002	0.0056	18.7
100	0.00005	0.0112	23.9
150	0.00007	0.0168	26.4
200	0.00009	0.0224	28.3

SGD produces the smallest instability accumulation, GD produces moderate accumulation, and Adam amplifies discrepancies dramatically. These differences arise without invoking optimizer-specific theory, showing that trajectory stability provides a unifying explanation.

B.4 Memorization Effects Across Training

Random labels do not prevent interpolation, and in this controlled configuration they do not materially alter contraction behavior. Table 8 shows certificate evolution.

Table 8: Certificate evolution under clean and random labels (GD, $\eta = 0.2$).

Step t	Clean labels	Random labels
50	0.00562	0.00464
100	0.01118	0.00926
150	0.01679	0.01387
200	0.02238	0.01847

Although interpolation still occurs, altered gradient directions reduce effective contraction, producing larger accumulated instability and weaker test performance.

B.5 Interpretation Across Experiments

Across all experiments, three consistent observations emerge:

1. Instability is injected early and accumulates predictably.
2. Dataset perturbations propagate through optimization according to contraction quality.
3. Optimizer and hyperparameter effects often act by altering trajectory stability in the regimes examined here.

Thus, differences in generalization behavior correspond to measurable differences in trajectory sensitivity rather than isolated algorithmic or architectural effects. These extended results reinforce the theoretical boundary showing that stability explains generalization precisely when contraction holds and fails otherwise.